DOI: 10.24352/UB.OVGU-2017-065 TECHNISCHE MECHANIK, 34, 3-4, (2014), 233 – 245
submitted: October 16, 2013

Elastic State Induced Energy Gap Variation in ZnTe/ZnMgTe Core/Shell Nanowires

R. Wojnar, P. Wojnar, S. Kret

The zinc telluride (ZnTe) nanowires grown recently are covered with the ZnMgTe shell. As a result of addition of magnesium the ZnMgTe lattice is expanded with respect to pure ZnTe lattice. From the lattice mismatch between the ZnMgTe shell and ZnTe nanowire core the internal strain and stress are created. Depending on the shell thickness and the Mg content in the shell the optical emission exhibits a considerable energy shift. To estimate this effect, at least qualitatively, the elastic state of the nanowire is calculated.

An analysis of the state of strain and stress in the core-shell nanowire within linear elasticity, using an analogy with thermal stresses is presented, in the similar way as it is applied, e.g. in hygro-mechanics. The suitable system of the differential Lamé-Navier's type equations is derived, and its solution for the axially symmetric problem is given. The jump of stress at the core-shell boundary is determined.

1 Introduction

In solid-state physics, an energy gap (band gap) means an energy interval in the energy spectrum of the solid, in which no electron states can exist. Substances with large energy gap are insulators, those with the smaller one are semiconductors, and when the gap is very small or none we are dealing with conductors. The energy gap of a material can be changed by controlling the composition of certain semiconductor alloys. For example, it is possible to build, as we do, the layered materials with alternating compositions by techniques of molecular–beam epitaxy. In general, the energy gap of semiconductors is decreasing with increase of the temperature. Energy gaps is depending also on the mechanical stress, and here is the motivation of this paper, cf. Kittel (2005).

Optical properties of semiconductor nanowires attract a great interest because of emerging applications of these structures in the field of nano-photonics and photovoltaics (Sköld et al., 1983; Waag et al., 1993; Ghosh et al., 2009; Soykan et al., 2010). Te-based nanowires are especially promising in this respect because II-VI semiconductors are characterized by direct energy gaps with values covering the entire visible light spectral range, from 1.6 eV (CdTe) to 3.5 eV (MnTe). Recently ZnTe nanowires embedded in ZnMgTe coating shells are fabricated using gold catalyst assisted molecular beam epitaxy (Ghosh et al., 2009). An intense emission from the nanowire cores at energies corresponding to the energy gap of ZnTe is observed.

Zinc telluride typically has a regular (cubic) crystal structure of the zincblende type, (Soykan et al., 2010). ZnTe can be easily doped, and for this reason it is one of the more common semiconducting materials used in optoelectronics, (Ghosh et al., 2009). When doped with the magnesium atoms it creates the ZnMgTe alloy. An enhancement of the Zeeman splitting as a result of the incorporation of paramagnetic Mn ions in ZnMnTe/ZnMgTe core/shell nanowires is observed, (Wojnar et al., 2012). One can compare the atomic radii of the atoms of the alloy: $^{52}_{127.6}$Te - 140 pm $^{30}_{65.4}$Zn - 134 pm $^{12}_{24.3}$Mg - 160 pm and observe that the radius of magnesium is the greatest despite of the lowest atomic magnesium number.

The lattice constant of ZnMgTe crystal is estimated from the experimental relation

$$a_{\mathrm{ZnMgTe}} = \frac{1}{5}\, a_{\mathrm{MgTe}} + \frac{4}{5}\, a_{\mathrm{ZnTe}}. \tag{1}$$

Both synthesised materials, ZnTe (core) and ZnMgTe (shell), have the same zinc blende cubic crystal structure, the same spacial orientation of crystal axes, but differ by the lattice constant. This is 6.1034$\mathring{A}$ in ZnTe, 6.42$\mathring{A}$ in MgTe (Landolt and Börnstein, 1982), and 6.17$\mathring{A}$ in ZnMgTe. The last value is obtained from Eq.(1). The difference

between the lattice constants of ZnTe and ZnMgTe leads to the mismatch between the lattices at the core and shell at the contact surface (the interface). The influence of introduction of the Mn-atom on the shell material constant can be regarded as a similar to the action of temperature, and this analogy will be exploited further.

1.1 The Core-Shell Nanowire

Depending on the thickness and the Mg content in the shell this emission exhibits a considerable energy shift. This effect can be at least qualitatively explained in terms of strain induced energy gap variation of the zinc telluride (ZnTe), whereas the strain originates from the lattice mismatch between the ZnMgTe nanowire shells and ZnTe nanowire cores. This interpretation is consistent with the experimental fact that the increase of the Mg content in the shell, as well as the increase of the thickness of the shell, which correspond both with the increase of the tensile strain in the nanowire cores, result in the red shift of the energy gap.

Hence, an analysis of the elastic state in the core-shell nanowire is needed. Calculations are made within the scope of linear elasticity, using an analogy with thermal stresses, in a similar way as it is applied, e.g., in hygro-elasticity (Ignaczak, 1978; Szekeres, 2012). A suitable system of the differential Lamé–Navier's type equations is derived, and its approximate solution is given.

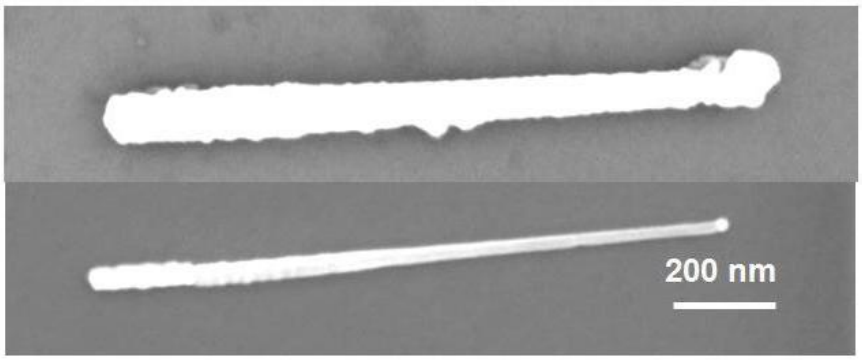

Figure 1. Nanowire with and without ZnMgTe shell. Average diameter of nanowires with shell: 81 ± 7nm, average diameter of nanowires without shell: 33 ± 9nm.

1.2 Bir-Pikus' Hamiltonian

Since the physics of a semiconductor is largely governed by the carriers in the extreme points of energy bands, Bir and Pikus (1974) observed that only the neighbourhoods of the band extrema are important and that the qualitative properties of these materials are governed by the shape of these energy surfaces. For the regular crystal the Hamiltonian, in which the strain components are included is as follows

$$\mathcal{H}_{BP} = \left(\frac{5}{4}\,b - a\right) \sum_i \varepsilon_{ii} - b \sum_i \varepsilon_{ii}\, J_i^2 - \frac{d}{\sqrt{3}} \left[\varepsilon_{xy}\left(J_x J_y + J_y J_x\right) + \text{c.p.}\right]$$

where ε_{ij}, $i = 1, 2, 3 \equiv x, y, z$ are the strain tensor components, J_i are the components of the angular momentum, and a, b and d are the constants (Landolt and Börnstein, 1982)

$$a = 5.47\text{eV} \qquad b = 1.26\text{eV} \qquad d = 4.2\text{eV}.$$

As the spin-orbit coupling is an interaction of a particle's spin with its motion described by the angular momentum, the Hamiltonian has the matrix form

$$\mathcal{H}_{BP} = \left\{ \begin{array}{cccc} P-Q & R & 0 & 0 \\ R^* & P+Q & 0 & 0 \\ 0 & 0 & P+Q & R \\ 0 & 0 & R^* & P-Q \end{array} \right\}$$

with

$$P = -\sum_i \varepsilon_{ii} \equiv -\left(\varepsilon_{xx} + \varepsilon_{yy} + \varepsilon_{zz}\right) \qquad Q = b\left(\varepsilon_{zz} - \frac{\varepsilon_{xx} + \varepsilon_{yy}}{2}\right) \qquad R = i\,d\,\varepsilon_{xy} - b\,\frac{\sqrt{3}}{2}\left(\varepsilon_{xx} - \varepsilon_{yy}\right)$$

and $i \equiv \sqrt{-1}$.

1.3 Regular (Cubic) Crystals and Matrix of Elasticity Tensor

The nanowire atomic structure has been observed by the high-resolution transmission electron microscopy (HR-TEM) which allows for direct imaging of the atomic structure of the sample.

High-resolution transmission electron microscopy (HR-TEM) is used for direct imaging of the atomic structure of the sample. The crystallographic features of a diametrical longitudinal cross-section of a nanowire are seen in Fig. 2, where the atomic lattice of a regular structure is visible.

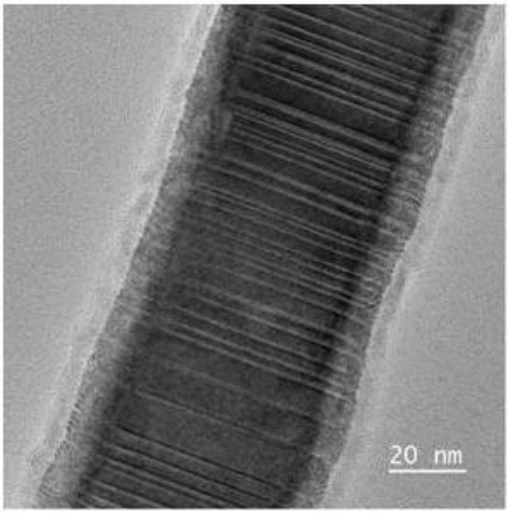

Figure 2. HR-TEM crystallographic structure: the diametrical longitudinal cross-section of a nanowire.

The elasticity coefficients for the regular crystal in the tensorial and Voigt's notation are given by the matrices

$$\begin{Bmatrix} c_{1111} & c_{1122} & c_{1122} & 0 & 0 & 0 \\ c_{1122} & c_{1111} & c_{1122} & 0 & 0 & 0 \\ c_{1122} & c_{1122} & c_{1111} & 0 & 0 & 0 \\ 0 & 0 & 0 & c_{2323} & 0 & 0 \\ 0 & 0 & 0 & 0 & c_{2323} & 0 \\ 0 & 0 & 0 & 0 & 0 & c_{2323} \end{Bmatrix} \equiv \begin{Bmatrix} C_{11} & C_{12} & C_{12} & 0 & 0 & 0 \\ C_{12} & C_{11} & C_{12} & 0 & 0 & 0 \\ C_{12} & C_{12} & C_{11} & 0 & 0 & 0 \\ 0 & 0 & 0 & C_{44} & 0 & 0 \\ 0 & 0 & 0 & 0 & C_{44} & 0 \\ 0 & 0 & 0 & 0 & 0 & C_{44} \end{Bmatrix}$$

and the matrix of coefficients of thermal expansion is

$$\begin{Bmatrix} \alpha & 0 & 0 \\ 0 & \alpha & 0 \\ 0 & 0 & \alpha \end{Bmatrix}$$

The regular crystal is characterised by 3 elasticity constants and one coefficient of thermal expansion.

1.4 The Aim of the Paper

The aim of this work is to confirm quantitatively, whether the observed energy gap variation as large as 80 meV can be attributed to strain effects only, or some additional effects such as, e.g., intrinsic electric fields.

To find the state of deformation of this system a continuous medium approximation is applied, and to determine the strain and stress fields a thermoelastic analogy is proposed. Namely, to account the difference of lattice constants, the structure is considered as a homogeneous one, but subject to a hypothetical non-homogeneous thermal field. First, the realistic cubic anisotropy of the medium is accounted for and the generalized displacement, Navier's type equation is derived. Further, since the material constants of both materials, of core and shell, are similar within 3% error, both materials are treated as isotropic, and a problem of an elastic cylinder in non-homogeneous thermal field with axial symmetry is considered. The continuity of suitable displacement and stress fields at the interface is assumed. In this approach the deformation field in the cross-section of the core is found uniform in agreement with the experiment.

2 Material Properties of the Nanowire Components

The measured material data of the nanowire components (Landolt and Börnstein, 1982) are given in the following table:

Table 1

material	function	a	$c_{1111} \equiv C_{11}$	$c_{1122} \equiv C_{12}$	$c_{2323} \equiv C_{44}$
		Å	GPa	GPa	GPa
Zn Te	CORE (A)	6.103	71.1	40.7	31.3
Mg Te		6.42	62.0	32.9	32.0
Zn Mg Te	SHELL (B)	6.17	69.3	39.1	31.4

2.1 Lamé's Parameters and Engineering Coefficients ([GPa])

The relations between Voigt's coefficients C_{11}, C_{12} and C_{44} and Lamé's parameters are given in the first line. The second and the third lines relate Lamé's parameters with the engineering coefficients: the bulk modulus K, Young's modulus E and Poisson's ratio ν,

$$c_{11} = \lambda + 2\mu \qquad c_{12} = \lambda \qquad c_{44} = 2\tilde{\mu}$$
$$K = \lambda + \frac{2}{3}\mu \qquad E = \frac{3\lambda + 2\mu}{\lambda + \mu}\mu \qquad \nu = \frac{1}{2}\frac{\lambda}{\lambda + \mu} \qquad E = (1+\nu)2\mu$$
$$E = 3 \cdot \frac{3K\mu}{3K + \mu} \qquad \nu = \frac{1}{2}\frac{3K - 2\mu}{3K + \mu}.$$

The measured values of Lamé's parameters and engineering coefficients are given below

Table 2

material	function	$\lambda + 2\mu$	λ	2μ	$2\tilde{\mu}$	K	E	ν
		GPa	GPa	GPa	GPa	GPa	GPa	
ZnTe	CORE (A)	71.1	40.7	30.4	31.3	50.8	41.5	0.364
ZnMgTe	SHELL (B)	69.3	39.1	30.2	31.4	49.2	41.1	0.361

We observe that the elastic properties of the core and shell differ only slightly. In particular, the coefficients μ and $\tilde{\mu}$ are similar within 3% margin.

2.2 The Regular (Cubic) Crystal Elasticity

In the frame of linear elasticity the strain components u_{ij} are associated with the displacement components u_i, $i = 1, 2, 3$ by the relation, cf. Landau and Lifshitz (1986),

$$\varepsilon_{ij} = \frac{1}{2}\left(\frac{\partial u_i}{\partial x_j} + \frac{\partial u_j}{\partial x_i}\right). \tag{2}$$

The elastic law for the regular crystal in the presence of a temperature difference Θ is

$$\sigma_{11} = 2\mu\,\varepsilon_{11} + \lambda\,\varepsilon_{kk} - \beta\Theta$$
$$\sigma_{22} = 2\mu\,\varepsilon_{22} + \lambda\,\varepsilon_{kk} - \beta\Theta$$
$$\sigma_{33} = 2\mu\,\varepsilon_{33} + \lambda\,\varepsilon_{kk} - \beta\Theta$$
$$\sigma_{32} = 2\tilde{\mu}\,\varepsilon_{32} \qquad \sigma_{31} = 2\tilde{\mu}\,\varepsilon_{31} \qquad \sigma_{12} = 2\tilde{\mu}\,\varepsilon_{12}$$

where

$$\beta = K\,\alpha \quad \text{and} \qquad K = \lambda + \frac{1}{3}2\mu.$$

2.3 Equilibrium Equations for the Regular Crystal

The equilibrium equation $\sigma_{ij,j} = 0$ after substitution of the elastic law and the strain - displacement relation leads to Navier-Cauchy's type equations

$$\begin{aligned}
\tilde{\mu}\,\Delta u_1 + (\lambda + \tilde{\mu})\frac{\partial}{\partial x_1}\frac{\partial u_k}{\partial x_k} - \beta\frac{\partial \Theta}{\partial x_1} + 2(\mu - \tilde{\mu})\frac{\partial^2 u_1}{\partial x_1^2} &= 0 \\
\tilde{\mu}\,\Delta u_2 + (\lambda + \tilde{\mu})\frac{\partial}{\partial x_2}\frac{\partial u_k}{\partial x_k} - \beta\frac{\partial \Theta}{\partial x_2} + 2(\mu - \tilde{\mu})\frac{\partial^2 u_2}{\partial x_2^2} &= 0 \\
\tilde{\mu}\,\Delta u_3 + (\lambda + \tilde{\mu})\frac{\partial}{\partial x_3}\frac{\partial u_k}{\partial x_k} - \beta\frac{\partial \Theta}{\partial x_3} + 2(\mu - \tilde{\mu})\frac{\partial^2 u_3}{\partial x_3^2} &= 0
\end{aligned} \tag{3}$$

where

$$\Delta = \left(\frac{\partial^2}{\partial x_1^2} + \frac{\partial^2}{\partial x_2^2} + \frac{\partial^2}{\partial x_3^2} \right).$$

Equations (3) are equations of thermoelasticity for the regular crystal. The temperature difference Θ is regarded as a given function.

Further we shall deal with an isotropic thermoelastic approximation. For the isotropic body $\tilde{\mu} = \mu$, the constants λ and μ are the Lamé parameters.

3 Non-homogeneous Isotropic Cylinder

The core-shell nanowire is approximated by a composite of two concentric cylinders, A and B, the inner with radius R_1 and the exterior with the radius R_2, see Figure 3. The lattice constants of the core A differs slightly from the lattice constant of the shell B, and this difference will be modelled by the thermal expansion. The question arises what the distribution of strains and stresses is, especially at the A-B interface.

In our case the non-homogeneity of the cylinder is modelled by introduction of the constant thermal field to the shell part. For this reason our problem is different from the problem solved by Muskhelishvili (1977), who considered the case in which the temperature was not constant in the exterior region, but smoothly changed from the temperature T_1 at R_1 do T_2 at R_2, (section 62 of his monograph).

3.1 Plane Strain

We exploit the axial symmetry of our problem.

The cylindrical coordinates, r, φ, z for our case of the axial symmetry are introduced and the strain-displacement relations are

$$\varepsilon_{rr} = \frac{\partial u_r}{\partial r} \qquad \varepsilon_{\varphi\varphi} = \frac{u_r}{r} \qquad \varepsilon_{zz} = \frac{\partial u_z}{\partial z} = 0.$$

The last relation means that along the nanowire, the state of strain does not vary, and in particular, the displacement u_z does not depend on variable z. All other strain components vanish also.
The normal stress components are

$$\begin{aligned} \sigma_{rr} &= (\lambda + 2\mu)\varepsilon_{rr} + \lambda\varepsilon_{\varphi\varphi} - K\alpha\Theta \\ \sigma_{\varphi\varphi} &= (\lambda + 2\mu)\varepsilon_{\varphi\varphi} + \lambda\varepsilon_{rr} - K\alpha\Theta \\ \sigma_{zz} &= \lambda\left(\varepsilon_{rr} + \varepsilon_{\varphi\varphi}\right) - K\alpha\Theta. \end{aligned} \tag{4}$$

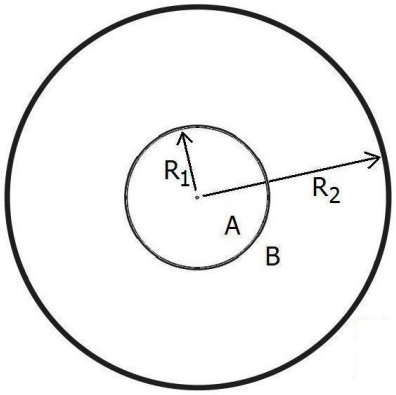

Figure 3. Schematic cross-section of the core-shell nanowire.

3.2 The Equilibrium Equation for the Isotropic Body

The equilibrium equation $\partial\sigma_{ij}/\partial x_j = 0$ expressed by the displacement u_i and the temperature Θ is

$$\mu\frac{\partial^2 u_i}{\partial x_j \partial x_j} + (\lambda+\mu)\frac{\partial^2 u_j}{\partial x_i \partial x_j} - K\alpha\frac{\partial\Theta}{\partial x_i} = 0 \tag{5}$$

or

$$(\lambda+2\mu)\frac{\partial^2 u_j}{\partial x_i \partial x_j} - \lambda\left(\operatorname{curl}\operatorname{curl}\mathbf{u}\right)_i - K\alpha\frac{\partial\Theta}{\partial x_i} = 0. \tag{6}$$

Because of the axial symmetry of our problem, the rotational term vanishes

$$\frac{\partial}{\partial x_i}\left\{(\lambda+2\mu)\frac{\partial u_j}{\partial x_j} - K\alpha\Theta\right\} = 0. \tag{7}$$

This equation will be analysed further.

4 Stress State

Let the temperature difference Θ in every part of the system, A and B, be constant, but not the same, taking the values Θ^A and Θ^B, respectively.
For the constant temperature Θ the equilibrium equation is

$$\nabla\operatorname{div}\mathbf{u} = 0 \tag{8}$$

and in the cylindrical system with axial symmetry

$$\frac{d}{dr}\operatorname{div}\mathbf{u} = 0.$$

Hence the radial displacement

$$u_r = \frac{1}{2}C_1 r + C_2\frac{1}{r}$$

the strains

$$u_{rr} = \frac{du_r}{dr} = \frac{1}{2}C_1 - C_2\frac{1}{r^2}$$

$$u_{\varphi\varphi} = \frac{u}{r} = \frac{1}{2}C_1 + C_2\frac{1}{r^2}$$

and, according to Eqs.(4), the stresses are

$$\sigma_{rr} = (\lambda+\mu)C_1 - 2\mu C_2\frac{1}{r^2} - K\alpha\Theta$$

$$\sigma_{\varphi\varphi} = (\lambda+\mu)C_1 + 2\mu C_2\frac{1}{r^2} - K\alpha\Theta$$

$$\sigma_{zz} = \lambda C_1 - K\alpha\Theta.$$

We introduce the notation

in part A

$$u_r^A = \frac{1}{2}C_1^A r + C_2^A\frac{1}{r}$$

and in part B

$$u_r^B = \frac{1}{2}C_1^B r + C_2^B\frac{1}{r}.$$

In the core (part A), where the value of radius $r = 0$ is possible, to avoid a singularity we should put $C_2^A = 0$.

Thus we obtain in the part A:
the strains

$$u_{rr}^A = \frac{1}{2} C_1^A$$

$$u_{\varphi\varphi}^A = \frac{1}{2} C_1^A$$

and the stresses

$$\sigma_{rr}^A = (\lambda^A + \mu^A) C_1^A - K^A \alpha^A \Theta^A$$

$$\sigma_{\varphi\varphi}^A = (\lambda^A + \mu^A) C_1^A - K^A \alpha^A \Theta^A$$

$$\sigma_{zz}^A = \lambda C_1^A - K^A \alpha^A \Theta^A.$$

In similar manner, for the Part B

$$u_{rr}^B = \frac{1}{2} C_1^B - C_2^B \frac{1}{r^2}$$

$$u_{\varphi\varphi}^B = \frac{1}{2} C_1^B + C_2^B \frac{1}{r^2}$$

and

$$\sigma_{rr}^B = (\lambda^B + \mu^B) C_1^B - 2\mu^B C_2^B \frac{1}{r^2} - K^B \alpha^B \Theta^B$$

$$\sigma_{\varphi\varphi}^B = (\lambda^B + \mu^B) C_1^B + 2\mu C_2^B \frac{1}{r^2} - K^B \alpha^B \Theta^B$$

$$\sigma_{zz}^B = \lambda C_1^B - K^B \alpha^B \Theta^B.$$

The integration constants are still unknown.

5 Evaluation of the Constants

Let $\Theta^A = 0$, $\alpha^B = \alpha$ and $\Theta^B = \Theta$.
At the external radius R_2 the normal component of stress $\sigma_{rr}^B = 0$. Hence

$$C_2^B = \frac{1}{2} \frac{R_2^2}{\mu^B} \left\{ (\lambda^B + \mu^B) C_1^B - K^B \alpha^B \Theta^B \right\}.$$

At the interface $r = R_1$ the following fields are continuous:
the normal stress components, hence

$$C_1^A = \left(\frac{R_2^2}{R_1^2} - 1 \right) \left\{ -\frac{\lambda^B + \mu^B}{\lambda^A + \mu^A} C_1^B + \frac{K^B}{\lambda^A + \mu^A} \alpha\Theta \right\}$$

and the displacement components, hence

$$\frac{1}{2} C_1^A R_1 = \frac{1}{2} C_1^B R_1 + C_2^B \frac{1}{R_1}$$

We eliminate the constants C_2^B and C_1^A and obtain

$$C_1^B = \frac{\left(\frac{R_2^2}{R_1^2} - 1 \right) \frac{K^B}{\lambda^A + \mu^A} + \frac{R_2^2}{R_1^2} \frac{K^B}{\mu^B}}{1 + \left(\frac{R_2^2}{R_1^2} - 1 \right) \frac{\lambda^B + \mu^B}{\lambda^A + \mu^A} + \frac{R_2^2}{R_1^2} \frac{\lambda^B + \mu^B}{\mu^B}} \alpha\Theta.$$

6 Our Model of the Cylinder

Assume that all elasticity constants in both components of the cylinder are the same, and the strain-stress state appears as a result of the difference of temperatures, Θ, only. Then we have

$$\lambda^A = \lambda^B = \lambda \qquad \mu^A = \mu^B = \mu \qquad \text{and} \qquad K^A = K^B = K.$$

As

$$\frac{K}{\mu} = \frac{2}{3} + \frac{\lambda}{\mu}$$

we have

$$C_1^B = \left\{1 + \left(1 - \frac{R_1^2}{R_2^2}\right) \frac{\mu}{\lambda + \mu}\right\} \frac{\lambda + \frac{2}{3}\mu}{\lambda + 2\mu}\, \alpha\Theta.$$

Moreover

$$C_2^B = \frac{1}{2} R_2^2 \left\{\left(1 + \frac{\lambda}{\mu}\right) C_1^B - \left(\frac{2}{3} + \frac{\lambda}{\mu}\right) \alpha\Theta\right\}$$

$$C_1^A = \left(\frac{R_2^2}{R_1^2} - 1\right) \left\{-C_1^B + \frac{\lambda + \frac{2}{3}\mu}{\lambda + \mu}\alpha\Theta\right\}.$$

These relations can be written equivalently

$$D \equiv K^B \alpha\, \Theta$$

$$C_1^B = \left\{1 + \left(1 - \frac{R_1^2}{R_2^2} \frac{\mu}{\lambda + \mu}\right)\right\} \frac{D}{\lambda + 2\mu}$$

$$C_1^A = \left(\frac{R_2^2}{R_1^2} - 1\right) \left(-\, C_1^B + \frac{D}{\lambda + \mu}\right)$$

$$C_2^B = \frac{1}{2}\, R_2^2 \left\{\left(1 + \frac{\lambda}{\mu}\right)\, C_1^B - \frac{D}{\mu}\right\}.$$

6.1 Elastic State in the Cylinder

Now we can write the expression for the stresses

$$\begin{aligned} \sigma_{rr}^A &= (\lambda + \mu) C_1^A \\ \sigma_{\varphi\varphi}^A &= (\lambda + \mu) C_1^A \\ \sigma_{zz}^A &= \lambda C_1^A \end{aligned} \tag{9}$$

and

$$\begin{aligned} \sigma_{rr}^B &= (\lambda + \mu) C_1^B - 2\mu C_2^B \frac{1}{r^2} - K\alpha^B\, \Theta \\ \sigma_{\varphi\varphi}^B &= (\lambda + \mu) C_1^B + 2\mu C_2^B \frac{1}{r^2} - K\alpha^B\, \Theta \\ \sigma_{zz}^B &= \lambda C_1^B - K\alpha^B\, \Theta. \end{aligned} \tag{10}$$

7 Numerical Example

For numerical calculations we introduce the engineering coefficients, and first, express the material constants in Eqs. (9) and (10) by Poisson's ratio ν

$$\frac{\mu}{\lambda+\mu} = 1-2\nu \qquad 1+\frac{\lambda}{\mu} = \frac{1}{1-2\nu}$$
$$\frac{\lambda}{\mu} = \frac{2\nu}{1-2\nu} \qquad \frac{\lambda+\frac{2}{3}\mu}{\lambda+2\mu} = \frac{1}{3}\,\frac{1+\nu}{1-\nu}$$
$$\frac{2}{3}+\frac{\lambda}{\mu} = \frac{2}{3}\,\frac{1+\nu}{1-2\nu} \qquad \frac{\lambda+\frac{2}{3}\mu}{\lambda+\mu} = \frac{2}{3}\,(1+\nu).$$

For the value of Poisson's ratio $\nu = 1/3$ we have

$$\frac{\mu}{\lambda+\mu} = \frac{1}{3} \qquad 1+\frac{\lambda}{\mu} = 3$$
$$\frac{\lambda}{\mu} = 2 \qquad \frac{\lambda+\frac{2}{3}\mu}{\lambda+2\mu} = \frac{2}{3}$$
$$\frac{2}{3}+\frac{\lambda}{\mu} = \frac{8}{3} \qquad \frac{\lambda+\frac{2}{3}\mu}{\lambda+\mu} = \frac{8}{9}.$$

The bulk modulus K for this value of ν equals Young's modulus

$$K = \frac{1}{3}\,\frac{E}{1-2\nu} = E \tag{11}$$

and

$$2\mu = \frac{3}{4}E. \tag{12}$$

Moreover, for $\nu = 1/3$ and K = 50 GPa, cf. Table 2,

$$\lambda = 2\mu = \frac{3}{4}K = 37.5\text{GPa.} \qquad \text{and} \qquad \lambda+\mu = \frac{9}{8}K = \frac{9}{8}\cdot 50\,\text{GPa} = 56.25\,\text{GPa.}$$

According to the experimental results, cf. Fig.1, the average diameter of the core is 33 ± 9nm, and the average external diameter of the shell is 81 ± 7nm. For the sake of simplicity we assume that the diameter of the core is $2\,R_1 = 40\,\text{nm}$ and the external diameter of the shell $2\,R_2 = 80\,\text{nm}$. Hence

$$\frac{R_2}{R_1} = 2. \tag{13}$$

We get, in the part A

$$C_1^B = \frac{5}{6}\alpha\Theta \qquad C_2^B = -\frac{1}{3}\,R_1^2\,\alpha\Theta \qquad C_1^A = \frac{1}{6}\alpha\Theta,$$

the strains

$$\varepsilon_{rr}^A = \frac{1}{2}C_1^A = \frac{1}{12}\,\alpha\Theta \qquad \varepsilon_{\varphi\varphi}^A = \frac{1}{2}C_1^A = \frac{1}{12}\,\alpha\Theta$$

and the stresses

$$\sigma_{rr}^A = (\lambda+\mu)C_1^A = (\lambda+\mu)\frac{1}{6}\,\alpha\Theta = \frac{9}{8}E\cdot\frac{1}{6}\,\alpha\Theta = \frac{3}{16}\,E\alpha\Theta$$

$$\sigma_{\varphi\varphi}^A = (\lambda+\mu)C_1^A = (\lambda+\mu)\frac{1}{6}\,\alpha\Theta = \frac{9}{8}E\cdot\frac{1}{6}\,\alpha\Theta = \frac{3}{16}\,E\alpha\Theta$$

$$\sigma_{zz}^A = \lambda C_1^A = \lambda\frac{1}{6}\,\alpha\Theta = \frac{3}{4}E\cdot\frac{1}{6}\,\alpha\Theta = \frac{1}{8}\,E\alpha\Theta,$$

while in the part B, the strains

$$\varepsilon_{rr}^B = \frac{1}{2}C_1^B - C_2^B\frac{1}{r^2} = \left(\frac{5}{12} + \frac{1}{3}\,\frac{R_1^2}{r^2}\right)\alpha\Theta \qquad \varepsilon_{\varphi\varphi}^B = \left(\frac{5}{12} - \frac{1}{3}\,\frac{R_1^2}{r^2}\right)\alpha\Theta$$

and the stresses

$$\sigma_{rr}^B = (\lambda+\mu)C_1^B - 2\mu C_2^B\frac{1}{r^2} - K\alpha\Theta = \left\{\frac{5}{16} + \frac{1}{4}\frac{R_1^2}{r^2} - 1\right\}E\alpha\Theta$$

$$\sigma_{\varphi\varphi}^B = (\lambda+\mu)C_1^B + 2\mu C_2^B\frac{1}{r^2} - K\alpha\Theta = \left\{\frac{5}{16} - \frac{1}{4}\frac{R_1^2}{r^2} - 1\right\}E\alpha\Theta$$

$$\sigma_{zz}^B = \lambda C_1^B - K\alpha\Theta = \left(\frac{5}{8} - 1\right)E\alpha\Theta = -\frac{3}{8}\cdot E\alpha\Theta.$$

We observe that at the interface $r = R_1$ the displacements are continuous, $u_r^A = u_r^B$,

$$u_r^A = \frac{1}{12}R_1\alpha\Theta \quad \text{and} \quad u_r^B = \left(\frac{5}{12} - \frac{1}{3}\,\frac{R_1^2}{R_1^2}\right)R_1\alpha\Theta = \frac{1}{12}\,\alpha\,\Theta\,R_1 \tag{14}$$

as well as the strains

$$\varepsilon_{\varphi\varphi}^A = \varepsilon_{\varphi\varphi}^B = \frac{1}{12}\alpha\Theta. \tag{15}$$

This means the continuity of the radial displacements and the circumferential strains at the interface. Also, at $r = R_1$

$$\sigma_{rr}^A = \sigma_{rr}^B = \frac{3}{16}E\alpha\Theta \tag{16}$$

what means the continuity of the normal stress.

According to the Table 1 the mismatch of the core and shell lattices equals

$$\frac{a_{\mathrm{ZnMgTe}} - a_{\mathrm{ZnTe}}}{a_{\mathrm{ZnTe}}} = \frac{0.06\mathring{A}}{6.1\mathring{A}} = 1\% \tag{17}$$

Hence, for the estimation we take

$$\alpha\Theta = \frac{1}{100}. \tag{18}$$

For the ratio $\nu = 1/3$, according to Eq.(11) and the Table 2, the value of the bulk modulus $K = E = 50$ GPa

$$K\alpha\Theta \equiv E\alpha\Theta = \frac{1}{100}\cdot 50\mathrm{GPa} = \frac{1}{2}\,\mathrm{GPa}. \tag{19}$$

Hence, cf. Eq.(16), at $r = R_1$,

$$\sigma_{rr}^A = \sigma_{rr}^B = \frac{3}{16}E\alpha\Theta = \frac{3}{32}\,\mathrm{GPa} = 0.09375\,\mathrm{GPa} = 93.75\,\mathrm{MPa}. \tag{20}$$

Such stresses are arisen at the interface of the core and the shell.

8 Discussion of the State of Stress at the CORE / SHELL Interface

One can ask for the influence of the surface tension γ, if it exists in the solid state, on the state of the stress. Again we return to Eq.(8) and easily find that then in the whole cross-section of the body the uniform pressure p is prevailing

$$p = \gamma\,\frac{1}{R_2}. \tag{21}$$

By an analogy, for the silicon at 1400^{o}C, cf. Fujii et al. (1997), we get 800 mN/m, what for R_2 = 80 nm gives p = 10 Mpa, i.e., more than 9 times smaller than the result given by Eq.(20). By the superposition of the linear elasticity this stress does not change the termal stresses calculated above.

On the atomic level, because of the difference between the lattice constants in core A and shell B, at the boundary between A and B, the dislocations can arise, cf. Gleiter and Lissowski (1971).

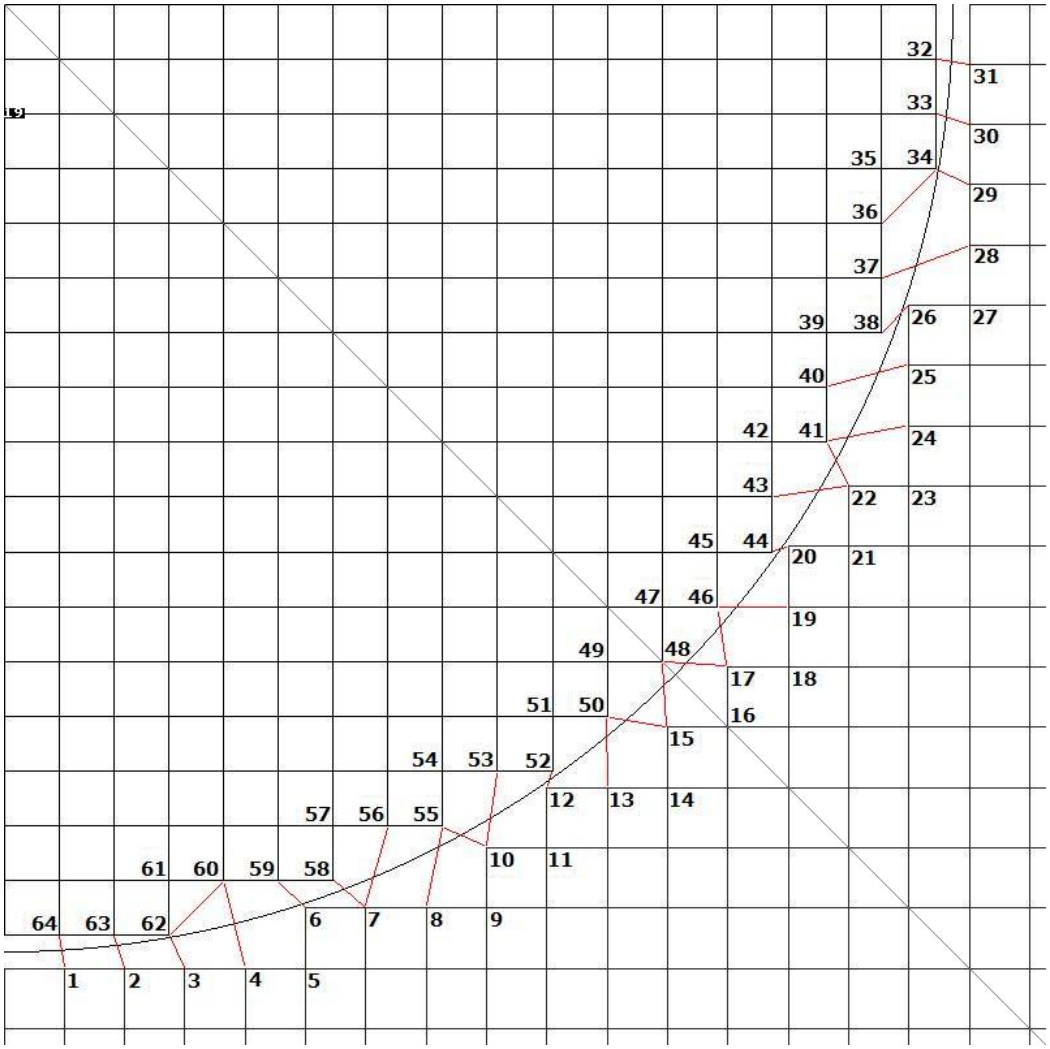

Figure 4. The mismatch of the crystallographic structures of ZnTe core and ZnMgTe shell, and appearance of the dislocations.

In Figure 4 the cross-section (a quarter only) of the cylinder is presented, for the case R_1 = 17 $\times 6.103\mathring{A} = 103.75\mathring{A}$, when the lattice constant is 10% greater than the lattice constant of the core. In such exaggerated scale, we observe two dislocation triangle-pentagon pairs only on the fourth part of the core-shell boundary. One pair is created by the triangle given by the atoms (60, 61, 62) and the pentagon given by the atoms (3, 4, 59, 60, 62) and the second (symmetrical) pair created by (34, 35, 36) and (28, 29, 34, 36, 37). From the interior part we have at the boundary 4 times 33 atoms and from the exterior part only 4 times 31 atoms.

Actually, in our case the number of atoms is greater, of order of 50, but the difference of both lattice constants is smaller, about 1%, cf. Section 2. So we cannot expect appearance of the dislocations, and the structure core-shell is safe from this side.

The other source of incertitude of the results lies in the estimation of the equivalent thermal expansion $\alpha\Theta$, corresponding to the substitution of the Zn atoms by the Mg atoms. Also the negligibility of the anisotropy may be the source of error. Thus, the results are provisional only. In next step the anisotropy of crystals should be accounted for, and the coefficient $\alpha\Theta$ ameliorated.

Acknowledgments

The research has been supported by the European Union within European Regional Development Fund through Innovative Economy grant (POIG.01.01.02-00-008/08), National Centre of Science (Poland) grant DEC-2011/01/D/ST5/05039 and Ministry of Higher Education (Poland) grant IP.

References

Bir, G. L.; Pikus, G. E.: *Symmetry and strain-induced effects in semiconductors*. John Wiley & Sons, New York (1974).

Fujii, H.; Matsumoto, T.; Nogi, K.: *Measurements of surface tension of molten silicon using electromagnetic levitation in drop shaft, in: Proceedings of the International Conference High Temperature Capillarity, 29 June 2 July 1997*. Edited by N. Eustathopoulos and N. Sobczak, Cracow (1997).

Ghosh, M.; Dilawar, N.; Bandyopadhyay, A. K.; Raychaudhuri, A. K.: Phonon dynamics of Zn(Mg,Cd)O alloy nanostructures and their phase segregation. *J. Appl. Phys.*, 106, (2009), 084306.

Gleiter, H.; Lissowski, A.: The rearrangement of atoms in high angle grain boundaries during grain boundary migration. *Z. Metallkunde*, 62, (1971), 237 – 239.

Ignaczak, J.: Tensorial equations of motion for a fluid saturated porous elastic solid. *Bull. Acad. pol. sci. Sér. sci. techn.*, 26, (1978), 371 – 375.

Kittel, C.: *Introduction to solid state physics (8th ed.)*. John Wiley & Sons, Hoboken, N.J. (2005).

Landau, L. D.; Lifshitz, E. M.: *Theory of elasticity (3rd ed.)*. Elsevier Butterworth-Heinemann, Amsterdam (1986).

Landolt, H.; Börnstein, R.: *Semiconductors, Physics of IV, III-V, II-VI and I-VII Compounds, Vol. III/17 B.*. Springer, Berlin (1982).

Muskhelishvili, N. I.: *Some basic problems of the mathematical theory of elasticity (3rd ed.)*. Noordhoff, Leyden (1977).

Sköld, N.; Karlsson, L. S.; Larsson, M. W.; Pistol, M.-E.; Seifert, W.; Trägårdh, J.; Samuelson, L.: Growth and optical properties of strained gaas-gaxin1-xp core-shell nanowires. *Nano Lett.*, 5, (1983), 1943–1947.

Soykan, C.; Ozdemir Kart, S.; Cagin, T.: Structural and mechanical properties of ZnTe in the zincblende phase. *Archives of Materials Science and Engineering, AMSE*, 46, (2010), 115 – 119.

Szekeres, A.: Cross-coupled heat and moisture transport: part 1 - theory. *J. Therm Stresses*, 35, (2012), 248 – 268.

Waag, A.; Heinke, H.; Schol, S. l.; Becker, C. R.; Landwehr, G.: Theories of immiscible and structured mixtures. *J. Cryst. Growth*, 131, (1993), 607 – 611.

Wojnar, P.; Janik, E.; Baczewski, L. T.; Kret, S.; Dynowska, E.; Wojciechowski, T.; Suffczyński, J.; Papierska, J.; Kossacki, P.; Karczewski, G.; Kossut, J.; Wojtowicz, T.: Giant spin splitting in optically active ZnMnTe/ZnMg Te core/shell nanowires. *Nano Lett.*, 12, (2012), 3404 – 3409.

Address: IPPT PAN, Warsaw, Poland
email: rwojnar@ippt.pan.pl; wojnar@ifpan.edu.pl; kret@ifpan.edu.pl